Bioorganic & Medicinal Chemistry 19 (2011) 5708–5715

Contents lists available at ScienceDirect

Bioorganic & Medicinal Chemistry

journal homepage: www.elsevier.com/locate/bmc

Synthesis, antibacterial activities and molecular docking studies of Schiff bases derived from *N*-(2/4-benzaldehyde-amino)phenyl-*N′*-phenyl-thiourea

Hong-Jia Zhang, Xuan Qin, Kai Liu, Di-Di Zhu, Xiao-Ming Wang *, Hai-Liang Zhu *

State Key Laboratory of Pharmaceutical Biotechnology, Nanjing University, Nanjing 210093, People's Republic of China

ARTICLE INFO

Article history:
Received 20 April 2011
Revised 24 June 2011
Accepted 25 June 2011
Available online 1 July 2011

Keywords:
Schiff base
Antibacterial activity
Structure–activity relationship
FabH inhibitors

ABSTRACT

A series of novel Schiff base derivatives have been designed and synthesized, and their biological activities were also evaluated as potential inhibitors of FabH. These compounds were assayed for antibacterial activity against *Escherichia coli*, *Pseudomonas aeruginosa*, *Bacillus subtilis* and *Staphylococcus aureus*. Compounds with potent antibacterial activities were tested for their *E. coli* FabH inhibitory activity. Compound **3v** showed the most potent antibacterial activity with MIC of 1.56–6.25 μg/mL against the tested bacterial strains and exhibited the most potent *E. coli* FabH inhibitory activity with IC_{50} of 4.3 μM. Docking simulation was performed to position compound **3v** into the *E. coli* FabH active site to determine the probable binding conformation.

1. Introduction

Although several classes of antibacterial agents are presently available, resistance in most of the pathogenic bacteria to these drugs constantly emerges. In order to prevent this serious medical problem, the elaboration of new types of antibacterial agents or the expansion of bioactivity of the previous drugs is a very important task.[1] Therefore, the research has been focused toward development of new antibacterial agents with novel target so as to surpass the problem of acquired resistance.

A promising target is the fatty acid synthase (FAS) pathway in bacteria. Fatty acid biosynthesis (FAB) is an essential metabolic process for prokaryotic organisms and is required for cell viability and growth.[2] β-Ketoacyl-acyl carrier protein (ACP) synthase III, also known as FabH or KAS III, plays an essential and regulatory role in bacterial FAB.[3,4] The enzyme initiates the fatty acid elongation cycles,[5,6] and is involved in the feedback regulation of the biosynthetic pathway via product inhibition.[7] FabH catalyzes the condensation reaction between a CoA-attached acetyl group and an ACP-attached malonyl group, yielding acetoacetyl-ACP as its final product (Fig. 1). Two other condensing enzymes, FabB (KASI) and FabF (KASII), perform the chain elongation reactions in subsequent cycles leading to longchain acyl ACP products,[8,9,3] while FabB and FabF are also condensing enzymes, FabH is structurally distinct.

FabH proteins from both Gram-positive and Gram-negative bacteria are highly conserved at the sequence and structural level while there are no significantly homologous proteins in humans. Importantly, the residues that comprise the active site are essentially invariant in various bacterial FabH molecules.[10–12] These attribute suggest that small molecule inhibitors of FabH enzymatic activity could be potential development candidates leading to selective, nontoxic and broad-spectrum antibacterials. Because of this, various kinds of compounds were screened by enzymatic assays to generate leads that were co-crystallized with various pathogenic FabH proteins and subsequently optimized using structure guided drug design methods.[13–17]

Some Schiff bases were reported to possess antibacterial, antifungal and antitumor activities.[18] Lots of researchers studied the synthesis, characterization and structure–activity relationship (SAR) of Schiff bases.[19–22] Kim and co-workers reported the YKAs3003, a Schiff base condensed by 4-hydroxy salicylaldehyde and cyclohexanamine as a potent inhibitor of *Escherichia coli* (*E. coli*) FabH with antimicrobial activity.[23] Further optimization of this compound is required to improve its antimicrobial activity.

Thiourea has been used as purification agent for the effluent of organic and inorganic, industrial, agricultural, and mining wastes.[24] This compound and its related analogues have become the focus of interest in recent past on account of their pharmacological activities, such as antidiabetic and antituberculosis.[25] Furthermore, thiourea has been studied for the systematic control of tuberculosis as well as anti-inflammatory activity during corrageenin induced edema in rats, while thiazoles and their ester possess depressant activity with central nervous system.[26] Recently, a few compounds of thiourea(2-amino-1,3-thiazines) have shown bactericidal, fungicidal, herbicidal, and algeacidal activities.[27] Importantly, it is reported that sulfur-urea-based Schiff base and its complexes exhibit excellent

* Corresponding authors. Tel.: +86 25 8359 2572; fax: +86 25 8359 2672.
E-mail address: zhuhl@nju.edu.cn (H.-L. Zhu).

0968-0896/$ - see front matter Crown Copyright © 2011 Published by Elsevier Ltd. All rights reserved.
doi:10.1016/j.bmc.2011.06.077

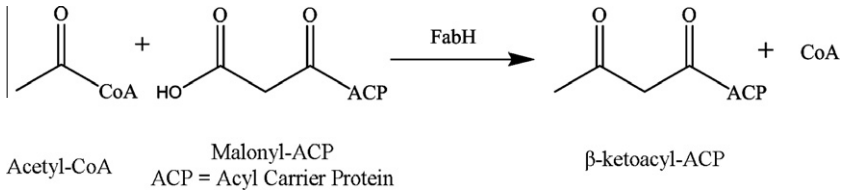

Figure 1. FabH-catalyzed ignition reaction of fatty acid biosynthesis.

antibacterial activity.[28–30] As a result, we hypothesized that Schiff base compounds containing thiourea skeleton may display potent antibacterial activity. In this study, we designed and synthesized a new series of Schiff bases derived from *N*-(2/4-benzaldehyde-amino) phenyl-*N*′-phenyl-thiourea and studied their antibacterial activities and *E. coli* FabH inhibitory activities. Docking simulations were performed using the X-ray crystallographic structure of the FabH of *E. coli* in complex with the most potent inhibitor to explore the binding modes of these compounds at the active site.

2. Results and discussion

2.1. Chemistry

In the present study, 12 benzaldehydes and 4 salicylaldehydes were subjected to react with 2 amines to prepare the corresponding Schiff bases (Scheme 1).

2.2. Biological activity

2.2.1. Antibacterial activity

All the synthesized compounds were screened for antibacterial activity against two Gram-negative bacterial strains:*Escherichia coli* (*E. coli*) and *Pseudomonas aeruginosa* (*P. aeruginosa*) and two Gram-positive bacterial strains: *Bacillus subtilis* (*B. subtilis*) and *Staphylococcus aureus* (*S. aureus*) by MTT method.[31] The MICs (minimum inhibitory concentrations) of the compounds against these bacteria were presented in Table 1. Also included was the activity of reference compound kanamycin. The results revealed that most of the synthesized compounds exhibited significant antibacterial activities.

Out of the 22 synthetic new Schiff bases, compound **3v**, (*E*)-1-(4-(4-(benzyloxy)benzylideneamino)phenyl)-3-phenylthiourea, exhibited the most potent antibacterial activity with MIC of 1.56, 3.13, 6.25 and 3.13 μg/mL against *E. coli*, *P. aeruginosa*, *B. subtilis* and *S. aureus*, respectively, which was similar to the broad-spectrum antibiotic Kanamycin B with corresponding MIC of 1.56, 3.13, 0.39 and 3.13 μg/mL and Penicillin G with corresponding MIC of 3.13, 6.25, 1.56 and 6.25 μg/mL.

As shown in Table 1, compounds **3a**–**3g** were condensed by *o*-aniline and substituted salicylaldehydes and benzaldehydes, while compounds **3h**–**3v** were condensed by *p*-aniline and substituted salicylaldehydes and benzaldehydes. Various substituents of aldehyde such as hydroxyl, halogen, methyl, methoxyl and nitro group lead to the different antibacterial activities of these Schiff bases, as well as the position of aniline. Based on the data obtained, we found that compounds **3h**–**3v** with *p*-aniline showed better antibacterial activity than those that compounds **3a**–**3g** with *o*-aniline. Besides, compounds with halogen group on salicylaldehyde and benzaldehyde component exhibited moderate activity with MIC of 3.13 to more than 100 μg/mL. Among them, compounds **3c**, **3j**, **3n** and **3r** with chloro group on aldehyde component showed

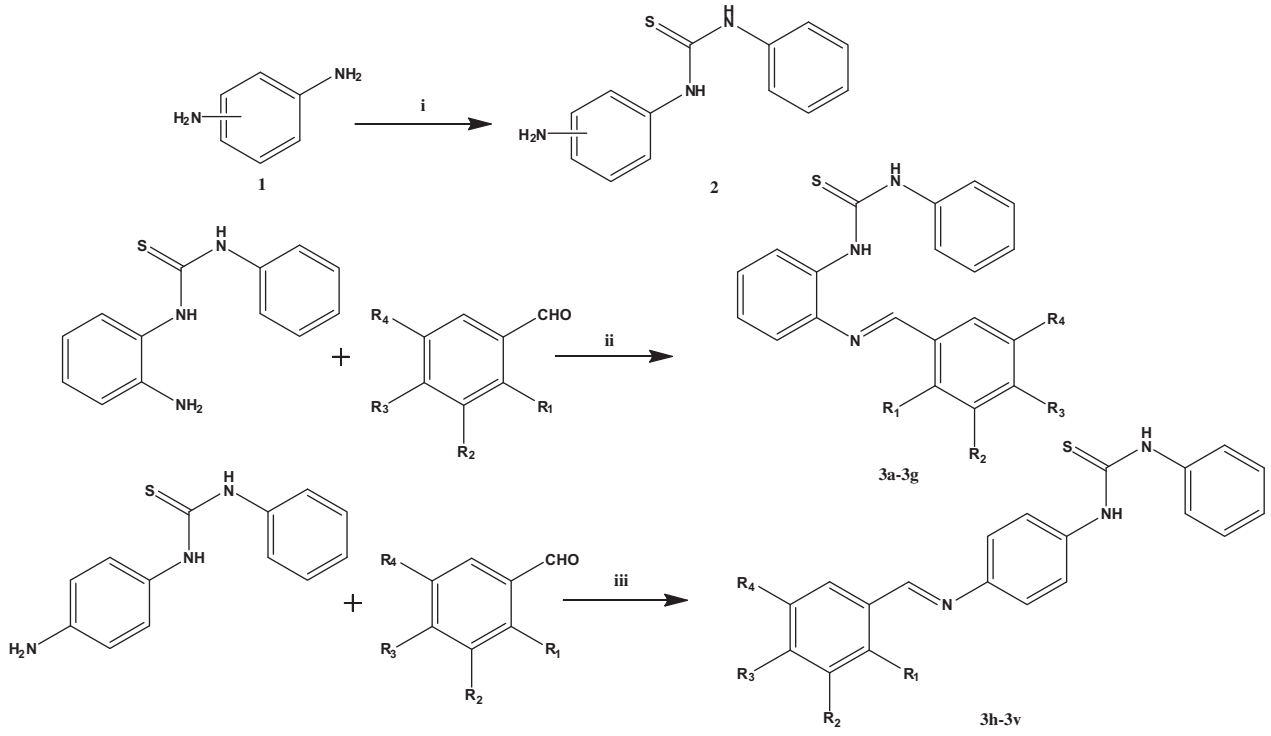

Scheme 1. General synthesis of *N*-(2/4-salicylaldehyde-amino) phenyl-*N*′-phenyl-thiourea and *N*-(2/4-benzaldehyde-amino) phenyl-*N*′-phenyl-thiourea derivatives (**3a**–**3v**). Reagents and conditions: (i) PhNCS, EtOH, 20 °C, 1–2 h; (ii) EtOH, 80 °C, 2.5 h or toluene, *p*-toluenesulfonic acid, 80 °C, 3–4 h; (iii) EtOH, 80 °C, 2.5 h or toluene, *p*-toluenesulfonic acid, 80 °C, 3–4 h.

Table 1
Structure of *N*-(2/4-salicylaldehyde-amino) phenyl-*N*′-phenyl-thiourea and *N*-(2/4-benzaldehyde-amino) phenyl-*N*′-phenyl-thiourea derivatives (**3a**–**3v**)

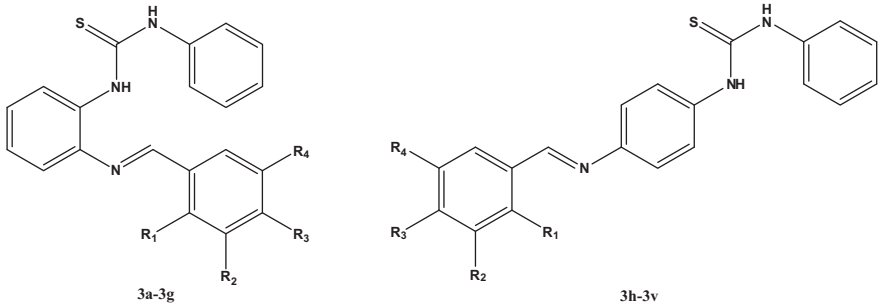

Compound	R_1	R_2	R_3	R_4
3a	OH	H	H	H
3b	OH	Br	H	Br
3c	OH	H	H	Cl
3d	OH	H	H	Br
3e	H	H	Cl	H
3f	H	H	Br	H
3g	H	H	OCH_3	H
3h	OH	H	H	H
3i	OH	Br	H	Br
3j	OH	H	H	Cl
3k	OH	H	H	Br
3l	F	H	H	H
3m	NO_2	H	H	H
3n	Cl	H	Cl	H
3o	H	Br	H	H
3p	H	OCH_3	H	H
3q	H	H	F	H
3r	H	H	Cl	H
3s	H	H	Br	H
3t	H	H	NO_2	H
3u	H	H	CH_3	H
3v	H	H	OCH_2Ar	H

better antibacterial activity with MIC of 3.13–25 μg/mL against the tested bacterial strains. However, compound **3e** with *p*-substituted chloro group lead to the great decrease of antibacterial activity. These results demonstrated that hydroxyl group on aldehyde is not conducive to the antibacterial activity of synthetic Schiff bases. This can also be seen from the result compared with **3e** and **3r**, **3f** and **3s**, respectively. Compounds **3m** and **3t** with nitro group showed weak antibacterial activity.

2.2.2. *E. coli* FabH inhibitory activity

The *E. coli* FabH inhibitory potency of the synthetic Schiff bases with potent antibacterial activities (**3b**, **3h**, **3j**, **3k**, **3n**, **3p**, **3r**, **3s**, **3u** and **3v**) was examined and the results are summarized in Table 3. Most of the tested compounds displayed potent *E. coli* FabH inhibitory. Among them, compound **3v** condensing by 4-(benzyloxy)benzaldehyde and 1-(4-aminophenyl)-3-phenylthiourea showed the most potent inhibitory with IC_{50} of 4.3 μM. This result supported the potent antibacterial activities of **3v**. It also indicated that compounds **3c**, **3h**, **3j** and **3k** which were condensed by salicylaldehyde and substituented amines showed moderate *E. coli* FabH inhibitory activity with IC_{50} of 9.5–39.0 μM. Among them, compound **3c** reacted with *o*-amine exhibited better inhibitory activity than those reacted with *p*-amine. As shown in Table 2, compound **3p** with *m*-substituented displayed worst inhibitory activity. Compound **3k** and **3s** were found to be inactive against *E. coli* FabH. This indicated that Schiff bases with bromine-substituted on aldehyde lead to the decrease of *E. coli* FabH inhibitory activity.

The results of *E. coli* FabH inhibitory activity of the test compounds were corresponding to the structure relationships (SAR) of their antibacterial activities. This demonstrated that the potent antibacterial activities of the synthetic compounds were probably correlated to their FabH inhibitory activities.

2.3. Binding model of compound 3v and *E. coli* FabH

Molecular docking of compound **3v** and *E. coli* FabH was performed on the binding model based on the *E. coli* FabH-CoA complex structure (1HNJ.pdb).[32] The FabH active site generally contains a catalytic triad tunnel consisting of Cys-His-Asn, which is conserved in various bacteria. This catalytic triad plays an important role in the regulation of chain elongation and substrate binding. Since the alkyl chain of CoA is broken by Cys of the catalytic triad of FabH, interactions between Cys and substrate appear to play an important role in substrate binding. Qiu et al. have refined three-dimensional structure of *E. coli* FabH in the presence and absence of malonyl-CoA by X-ray spectroscopy. Since malonyl moiety is degraded by *E. coli* FabH, molecular docking studies for FabH and malonyl-CoA was carried out to identify a plausible malonyl-binding mode.[32] They found that in one of the binding modes appeared in the lower scored conformations, the malonyl carboxylate formed hydrogen bonds to the backbone nitrogen of Phe304.

The binding model of compound **3v** and *E. coli* FabH is depicted in Figure 2. It can be seen from Figure 2 that, in the binding model of compound **3v** and *E. coli* FabH, there is one hydrogen bond.

Table 2
Antibacterial activity of synthetic compounds

Compounds	Minimum inhibitory concentrations (μg/mL)			
	Gram-negative		Gram-positive	
	E. coli ATCC35218	*P. aeruginosa* ATCC13525	*B. subtilis* ATCC6633	*S. aureus* ATCC6538
3a	>100	>100	>100	>100
3b	>100	>100	>100	>100
3c	3.13	3.13	12.5	6.25
3d	>100	>100	>100	>100
3e	>100	>100	>100	>100
3f	>100	>100	50	>100
3g	>100	>100	>100	>100
3h	12.5	6.25	25	6.25
3i	>100	>100	>100	>100
3j	6.25	6.25	12.5	12.5
3k	25	25	50	50
3l	>100	>100	>100	>100
3m	>100	>100	50	25
3n	12.5	25	12.5	12.5
3o	>100	>100	>100	>100
3p	50	25	25	50
3q	50	50	50	25
3r	6.25	3.13	12.5	6.25
3s	25	25	50	50
3t	25	50	50	50
3u	12.5	25	25	25
3v	1.56	3.13	6.25	3.13
Kanamycin B	1.56	3.13	0.39	3.13
Penicillin G	3.13	6.25	1.56	6.25

Table 3
E. coli FabH inhibitory activity of synthetic compounds

Compounds	*E. coli* FabH IC_{50} (μM)	Hemolysis LC (mg/mL)
3c	9.5	>10
3h	28.7	>10
3j	12.8	>10
3k	39.0	>10
3n	30.4	>10
3p	48.1	>10
3r	15.6	>10
3s	40.8	>10
3u	25.9	>10
3v	4.3	>10

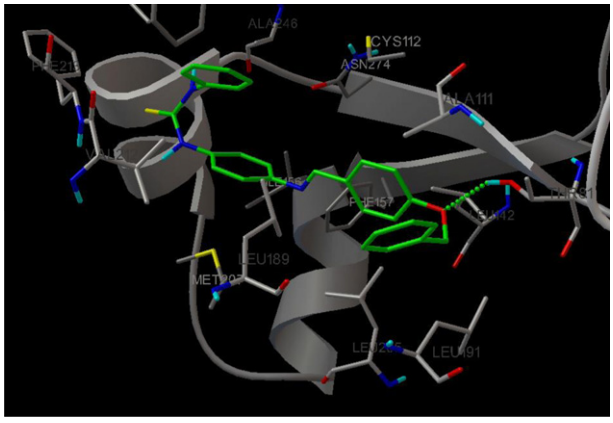

Figure 2. Binding model of compound **3v** (colored in green) into *E. coli* FabH. H-bond is shown as dotted green lines. THR81 forms hydrogen bond with the oxygen atom of compound **3v**.

THR81 forms hydrogen bond with the oxygen atom of compound **3v**. The result along with the data of *E. coli* FabH inhibitory activity assay indicated that compound **3v** would be potential inhibitors of *E. coli* FabH with potent antibacterial activity.

3. Conclusions

A series of novel Schiff bases reacting by *N*-(2/4-benzaldehyde-amino) phenyl-*N*′-phenyl-thiourea and substituted benzaldehyde and salicylaldehyde were synthesized and assayed for their antibacterial activities against *E. coli*, *P. fluorescence*, *B. subtilis* and *S. aureus*. Compound **3v**, (*E*)-1-(4-(4-(benzyloxy)benzylideneamino)phenyl)-3-phenylthiourea showed the most potent antibacterial activity with MIC of 1.56–6.25 μg/mL against the test bacterial strains and exhibited the most potent *E. coli* FabH inhibitory activity with IC_{50} of 4.3 μM, which was compared with the positive control Kanamycin B and Penicillin G. Docking simulation was performed to position compound **3v** into the *E. coli* FabH active site to determine the probable binding conformation. Analysis of the compound **3v**'s binding conformation in active site displayed the compound **3v** was stabilized by hydrogen bonding interactions with THR81. Antibacterial assay results also showed that these Schiff base derivatives had the potential to be developed for antibacterial agents against *E. coli*. Particularly, compound **3v** has demonstrated significant *E. coli* FabH inhibitory activity as a potential antibacterial agent.

4. Experiments

4.1. Materials and measurements

All chemicals and reagents used in current study were analytical grade. All the ^{1}H NMR spectra were recorded on a Bruker DPX 300 model Spectrometer in DMSO-d_6 and chemical shifts were reported in ppm (δ). ESI-MS spectra were recorded on a Mariner System 5304 Mass spectrometer. Elemental analyses were performed on a CHN-O-Rapid instrument. TLC was performed on the glass-backed silica gel sheets (silica gel 60 Å GF254) and visualized in UV light (254 nm). All the compounds gave satisfactory chemical analyses (±0.4%). ^{1}H NMR and ESI-MS spectra were consistent with the assigned structures.

4.2. General procedure for synthesis of *N*-(2/4-amino) phenyl-*N*′-phenyl-thiourea

o-Diaminobenzene or *p*-diaminobenzene (1.85 mmol) was dissolved in ethanol (4 mL) and stirred 20 °C, a solution of phenyl isothiocyanate (0.22 mL) and ethanol was dropwised into the reaction mixture when the diaminobenzene was completely dissolved. The reaction mixture was stirred until the solids formed largely. The products were filtrated and washed carefully with EtOH; the resulting *N*-(2/4-amino) phenyl-*N*′-phenyl-thiourea were purified by crystallization from EtOH in refrigerator (Scheme 1).

4.3. General procedure for synthesis of *N*-(2/4-salicylaldehyde-amino) phenyl-*N*′-phenyl-thiourea derivatives

N-(2/4-Amino) phenyl-*N*′-phenyl-thiourea (2.5 mmol) was dissolved in ethanol (10 mL) and stirred 80 °C, salicylaldehyde (3.0 mmol) was dropwised into the solution when the solid was completely dissolved. The reaction mixture was stirred for 2.5 h. The products were filtrated timely and dried by vacuum (Scheme 1).

4.3.1. (*E*)-1-(2-(2-hydroxybenzylideneamino)phenyl)-3-phenylthiourea (3a)

Yellow crystals, yield 81%, mp: 216–218 °C, ^{1}H NMR (300 MHz, DMSO-d_6, δ ppm): 6.95–6.99 (m, 2H), 7.12 (t, J = 7.40 Hz, 1H), 7.28–7.33 (m, 4H), 7.37–7.46 (m, 4H), 7.63–7.66 (m, 2H), 8.88 (s, 1H), 9.49 (s, 1H), 9.90 (s, 1H), 12.66 (s, 1H, OH). ESI-MS: 348.1 ($C_{20}H_{18}N_3OS$, $[M+H]^+$). Anal. Calcd for $C_{20}H_{17}N_3OS$: C, 69.14; H, 4.93; N, 12.09. Found: C, 69.42; H, 5.21; N, 12.15.

4.3.2. (*E*)-1-(2-(3,5-Dibromo-2-hydroxybenzylideneamino)phenyl)-3-phenylthiourea (3b)

Yellow crystals, yield 78%, mp: 173–174 °C, ^{1}H NMR (300 MHz, DMSO-d_6, δ ppm): 7.13 (t, J = 7.32 Hz, 1H), 7.31 (t, J = 7.77 Hz, 2H), 7.35–7.41 (m, 2H), 7.47 (d, J = 8.04 Hz, 4H), 7.92 (dd, J_1 = 12.42 Hz, J_2 = 12.24 Hz, 2H), 8.92 (s, 1H), 9.51 (s, 1H), 9.90 (s, 1H), 14.39 (s, 1H, OH). ESI-MS: 503.9 ($C_{20}H_{16}Br_2N_3OS$, $[M+H]^+$). Anal. Calcd for $C_{20}H_{15}Br_2N_3OS$: C, 47.55; H, 2.99; N, 8.32. Found: C, 47.73; H, 3.25; N, 8.61.

4.3.3. (*E*)-1-(2-(5-Chloro-2-hydroxybenzylideneamino)phenyl)-3-phenylthiourea (3c)

Yellow crystals, yield 80%, mp: 190–192 °C, ^{1}H NMR (300 MHz, DMSO-d_6, δ ppm): 7.00 (d, J = 8.79 Hz, 1H), 7.12 (t, J = 7.32 Hz, 1H), 7.28–7.34 (m, 5H), 7.42–7.46 (m, 3H), 7.69 (t, J = 4.45 Hz, 1H), 7.77 (d, J = 2.55 Hz, 1H), 8.86 (s, 1H), 9.45 (s, 1H), 9.91 (s, 1H), 12.54 (s, 1H, OH). ESI-MS: 382.1 ($C_{20}H_{17}ClN_3OS$, $[M+H]^+$). Anal. Calcd for $C_{20}H_{16}ClN_3OS$: C, 62.90; H, 4.22; N, 11.00. Found: C, 63.14; H, 4.33; N, 12.14.

4.3.4. (*E*)-1-(2-(5-Bromo-2-hydroxybenzylideneamino)phenyl)-3-phenylthiourea (3d)

Yellow crystals, yield 83%, mp: 197–198 °C, ^{1}H NMR (300 MHz, DMSO-d_6, δ ppm): 6.95 (d, J = 8.79 Hz, 1H), 7.12 (t, J = 7.32 Hz, 1H), 7.28–7.34 (m, 5H), 7.45 (d, J = 7.86 Hz, 2H), 7.55 (dd, J_1 = 8.79 Hz, J_2 = 8.79 Hz, 1H), 7.67 (t, J = 4.57 Hz, 1H), 7.90 (d, J = 2.55 Hz, 1H), 8.85 (s, 1H), 9.45 (s, 1H), 9.90 (s, 1H), 12.58 (s, 1H, OH). ESI-MS: 426.0 ($C_{20}H_{17}BrN_3OS$, $[M+H]^+$). Anal. Calcd for $C_{20}H_{16}BrN_3OS$: C, 56.34; H, 3.78; N, 9.86. Found: C, 56.61; H, 4.03; N, 10.14.

4.3.5. (*E*)-1-(4-(2-Hydroxybenzylideneamino)phenyl)-3-phenylthiourea (3h)

Yellow crystals, yield 76%, mp: 187–188 °C, ^{1}H NMR (300 MHz, DMSO-d_6, δ ppm): 6.95–7.01 (m, 2H), 7.14 (t, J = 7.41 Hz, 1H), 7.34 (t, J = 7.88 Hz, 2H), 7.38–7.44 (m, 3H), 7.50 (d, J = 8.04 Hz, 2H), 7.64 (d, J = 7.68 Hz, 1H), 8.97 (s, 1H), 9.86 (d, J = 12.45 Hz, 2H), 13.16 (s, 1H, OH). ESI-MS: 348.1 ($C_{20}H_{18}N_3OS$, $[M+H]^+$). Anal. Calcd for $C_{20}H_{17}N_3OS$: C, 69.14; H, 4.93; N, 12.09. Found: C, 69.38; H, 4.25; N, 12.16.

4.3.6. (*E*)-1-(4-(3,5-Dibromo-2-hydroxybenzylideneamino)phenyl)-3-phenylthiourea (3i)

Yellow crystals, yield 82%, mp: 286–289 °C, ^{1}H NMR (300 MHz, DMSO-d_6, δ ppm): 7.14 (t, J = 7.41 Hz, 1H), 7.35 (t, J = 7.86 Hz, 1H), 7.45–7.51 (m, 4H), 7.64 (t, J = 8.79 Hz, 2H), 7.90 (dd, J_1 = 17.37 Hz, J_2 = 17.37 Hz, 2H), 9.01 (s, 1H), 9.91 (d, J = 12.06 Hz, 2H), 14.74 (s, 1H, OH). ESI-MS: 503.9 ($C_{20}H_{16}Br_2N_3OS$, $[M+H]^+$). Anal. Calcd for $C_{20}H_{15}Br_2N_3OS$: C, 47.55; H, 2.99; N, 8.32. Found: C, 47.69; H, 3.14; N, 8.58.

4.3.7. (*E*)-1-(4-(5-Chloro-2-hydroxybenzylideneamino)phenyl)-3-phenylthiourea (3j)

Yellow crystals, yield 78%, mp: 206–209 °C, ^{1}H NMR (300 MHz, DMSO-d_6, δ ppm): 7.00 (d, J = 8.76 Hz, 1H), 7.14 (t, J = 7.32 Hz, 1H), 7.34 (t, J = 7.86 Hz, 2H), 7.39–7.45 (m, 3H), 7.49 (d, J = 7.68 Hz, 2H), 7.60 (d, J = 8.61 Hz, 2H), 7.74 (d, J = 2.73 Hz, 1H), 8.95 (s, 1H), 9.87 (d, J = 12.24 Hz, 2H), 13.10 (s, 1H, OH). ESI-MS: 382.1 ($C_{20}H_{17}ClN_3OS$, $[M+H]^+$). Anal. Calcd for $C_{20}H_{16}ClN_3OS$: C, 62.90; H, 4.22; N, 11.00. Found: C, 63.18; H, 4.47; N, 11.25.

4.3.8. (*E*)-1-(4-(5-Bromo-2-hydroxybenzylideneamino)phenyl)-3-phenylthiourea (3k)

Yellow crystals, yield 77%, mp: 211–212 °C, ^{1}H NMR (300 MHz, DMSO-d_6, δ ppm): 6.95 (d, J = 8.76 Hz, 1H), 7.14 (t, J = 7.32 Hz, 1H), 7.34 (t, J = 7.77 Hz, 2H), 7.41 (d, J = 8.79 Hz, 2H), 7.49 (d, J = 7.68 Hz, 2H), 7.52–7.56 (m, 1H), 7.60 (d, J = 8.61 Hz, 2H), 7.86 (d, J = 2.4 Hz, 1H), 8.95 (s, 1H), 9.87 (d, J = 12.06 Hz, 2H), 13.13 (s, 1H, OH). ESI-MS: 426.0 ($C_{20}H_{17}BrN_3OS$, $[M+H]^+$). Anal. Calcd for $C_{20}H_{16}BrN_3OS$: C, 56.34; H, 3.78; N, 9.86. Found: C, 59.42; H, 3.51; N, 9.75.

4.4. General procedure for synthesis of *N*-(2/4-benzaldehydeamino) phenyl-*N′*-phenyl-thiourea derivatives

Equimolar amount of *N*-(2/4-amino) phenyl-*N′*-phenyl-thiourea (1.63 mmol) and benzaldehyde (1.63 mmol) were dissolved in toluene, and *p*-toluenesulfonic acid (0.175 mmol) as a catalyst and stirred 80 °C for 3–4 h. The products were filtrated and washed carefully with ice water and cool EtOH; the products were purified by crystallization from EtOH in refrigerator (Scheme 1).

4.4.1. (*E*)-1-(2-(4-Chlorobenzylideneamino)phenyl)-3-phenyl thiourea (3e)

Yellow crystals, yield 80%, mp: 154–155 °C, ^{1}H NMR (300 MHz, DMSO-d_6, δ ppm): 7.18 (t, J = 7.59 Hz, 1H), 7.25 (d, J = 6.78 Hz, 1H), 7.31–7.42 (m, 4H), 7.46 (d, J = 8.04 Hz, 2H), 7.57 (d, J = 8.40 Hz, 2H), 7.80 (d, J = 8.61 Hz, 2H), 8.49 (d, J = 6.96 Hz, 1H), 8.72 (s, 1H), 9.46 (s, 1H), 10.23 (s, 1H). ESI-MS: 366.1 ($C_{20}H_{17}ClN_3S$, $[M+H]^+$). Anal. Calcd for $C_{20}H_{16}ClN_3S$: C, 65.65; H, 4.41; N, 11.48. Found: C, 65.95; H, 4.67; N, 11.66.

4.4.2. (*E*)-1-(2-(4-Bromobenzylideneamino)phenyl)-3-phenylthiourea (3f)

Yellow crystals, yield 84%, mp: 153–155 °C, ^{1}H NMR (300 MHz, DMSO-d_6, δ ppm): 7.17 (t, J = 7.58 Hz, 1H), 7.24–7.31 (m, 3H), 7.33–7.41 (m, 3H), 7.46 (d, J = 8.04 Hz, 2H), 7.69–7.75 (m, 3H), 8.49 (d, J = 8.04 Hz, 1H), 8.07 (s, 1H), 9.45 (s, 1H), 10.23 (s, 1H). ESI-MS: 410.0 ($C_{20}H_{17}BrN_3S$, $[M+H]^+$). Anal. Calcd for $C_{20}H_{16}BrN_3S$: C, 58.54; H, 3.93; N, 10.24. Found: C, 58.82; H, 4.16; N, 10.53.

4.4.3. (*E*)-1-(2-(4-Methoxybenzylideneamino)phenyl)-3-phenylthiourea (3g)

Yellow crystals, yield 82%, mp: 156–157 °C,^{1}H NMR (300 MHz, DMSO-d_6, δ ppm): 3.87 (s, 3H, OCH3), 7.04 (d, J = 8.79 Hz, 2H), 7.15–7.32 (m, 4H), 7.39 (t, J = 7.77 Hz, 2H), 7.46 (d, J = 8.07 Hz, 2H), 7.72 (d, J = 8.58 Hz, 2H), 8.54 (d, J = 6.57 Hz, 1H), 8.62 (s, 1H), 9.47 (s, 1H), 10.23 (s, 1H). ESI-MS: 362.1 ($C_{21}H_{20}N_3OS$, $[M+H]^+$). Anal. Calcd for $C_{21}H_{19}N_3OS$: C, 69.78; H, 5.30; N, 11.63. Found: C, 69.98; H, 5.52; N, 11.89.

4.4.4. (*E*)-1-(4-(2-Fluorobenzylideneamino)phenyl)-3-phenylthiourea (3l)

Yellow crystals, yield 79%, mp: 179–182 °C, ^{1}H NMR (300 MHz, DMSO-d_6, δ ppm): 7.13 (t, J = 7.31 Hz, 1H), 7.31–7.35 (m, 6H), 7.48–7.57 (m, 5H), 8.10 (t, J = 6.95 Hz, 1H), 8.80 (s, 1H), 9.84 (d, J = 14.25 Hz, 2H). ESI-MS: 350.1 ($C_{20}H_{17}FN_3S$, $[M+H]^+$). Anal. Calcd for $C_{20}H_{16}FN_3S$: C, 68.75; H, 4.62; N, 12.03. Found: C, 68.94; H, 4.94; N, 12.27.

4.4.5. (*E*)-1-(4-(2-Nitrobenzylideneamino)phenyl)-3-phenylthiourea (3m)

Yellow crystals, yield 77%, mp: 165–166 °C, ^{1}H NMR (300 MHz, DMSO-d_6, δ ppm): 7.13 (t, J = 7.96 Hz, 1H), 7.29–7.27 (m, 4H), 7.49 (d, J = 7.50 Hz, 2H), 7.57 (d, J = 8.79 Hz, 2H), 7.77 (t, J = 7.79 Hz, 1H), 7.88 (t, J = 7.50 Hz, 1H), 8.11 (d, J = 9.15 Hz, 1H), 8.19 (d, J = 9.15 Hz,1H), 8.90 (s, 1H), 9.85 (d, J = 16.29 Hz, 2H). ESI-MS: 377.1 ($C_{20}H_{17}N_4O_2S$, $[M+H]^+$). Anal. Calcd for $C_{20}H_{16}N_4O_2S$: C, 63.81; H, 4.28; N, 14.88. Found: C, 63.69; H, 4.47; N, 15.03.

4.4.6. (*E*)-1-(4-(2,4-Dichlorobenzylideneamino)phenyl)-3-phenylthiourea (3n)

Yellow crystals, yield 79%, mp: 184–185 °C, ^{1}H NMR (300 MHz, DMSO-d_6, δ ppm): 7.14 (t, J = 7.32 Hz, 1H), 7.32–7.37 (m, 4H), 7.49

(d, J = 7.86 Hz, 2H), 7.57 (d, J = 8.76 Hz, 3H), 7.79 (s, 1H), 8.17 (d, J = 8.61 Hz, 1H), 8.86 (s, 1H), 9.85 (d, J = 16.98 Hz, 2H). ESI-MS: 400.0 ($C_{20}H_{16}Cl_2N_3S$, $[M+H]^+$). Anal. Calcd for $C_20H_{15}Cl_2N_3S$: C, 60.00; H, 3.78; N, 10.50. Found: C, 60.34; H, 4.03; N, 10.68.

4.4.7. (*E*)-1-(4-(3-Bromobenzylideneamino)phenyl)-3-phenylthiourea (3o)

Yellow crystals, yield 75%, mp: 177–178 °C, ^{1}H NMR (300 MHz, DMSO-d_6, δ ppm): 7.13 (t, J = 7.32 Hz, 1H), 7.29–7.37 (m, 4H), 7.44–7.57 (m, 5H), 7.72 (d, J = 7.89 Hz, 1H), 7.93 (d, J = 7.86 Hz, 1H), 8.12 (s, 1H), 8.66 (s, 1H), 9.83 (d, J = 10.05 Hz, 1H). ESI-MS: 410.0 ($C_{20}H_{17}BrN_3S$, $[M+H]^+$). Anal. Calcd for $C_{20}H_{16}BrN_3S$: C, 58.54; H, 3.93; N, 10.24. Found: C, 58.84; H, 4.23; N, 10.38.

4.4.8. (*E*)-1-(4-(3-Methoxybenzylideneamino)phenyl)-3-phenylthiourea (3p)

Yellow crystals, yield 74%, mp: 250–253 °C, ^{1}H NMR (300 MHz, DMSO-d_6, δ ppm): 2.29 (s, 3H, OCH_3), 6.84 (s, 1H), 7.10–7.14 (m, 3H), 7.21 (d, J = 4.65 Hz, 1H), 7.31–7.34 (m, 2H), 7.44–7.50 (m, 5H), 7.54–7.55 (m, 1H), 8.66 (s, 1H), 9.80 (d, J = 11.87 Hz, 2H). ESI-MS: 362.1 ($C_{21}H_{20}N_3OS$, $[M+H]^+$). Anal. Calcd for $C_{21}H_{19}N_3OS$: C, 69.78; H, 5.30; N, 11.63. Found: C, 69.92; H, 5.54; N, 11.81.

4.4.9. (*E*)-1-(4-(4-Fluorobenzylideneamino)phenyl)-3-phenylthiourea (3q)

Yellow crystals, yield 81%, mp: 191–192 °C, ^{1}H NMR (300 MHz, DMSO-d_6, δ ppm): 7.13 (t, J = 7.32 Hz, 1H), 7.26–7.36 (m, 6H), 7.48–7.55 (m, 4H), 7.98–8.03 (m, 2H), 8.66 (s, 1H), 9.81 (d, J = 9.69 Hz, 2H). ESI-MS: 350.1 ($C_{20}H_{17}FN_3S$, $[M+H]^+$). Anal. Calcd for $C_{20}H_{16}FN_3S$: C, 68.75; H, 4.62; N, 12.03. Found: C, 68.89; H, 4.84; N, 12.21.

4.4.10. (*E*)-1-(4-(4-Chlorobenzylideneamino)phenyl)-3-phenylthiourea (3r)

Yellow crystals, yield 82%, mp: 187–188 °C, ^{1}H NMR (300 MHz, DMSO-d_6, δ ppm): 7.13 (t, J = 7.41 Hz, 1H), 7.28–7.37 (m, 4H), 7.48–7.61 (m, 6H), 7.96 (d, J = 8.4 Hz, 2H), 8.67 (s, 1H), 9.82 (d, J = 10.05 Hz, 2H). ESI-MS: 366.1 ($C_{20}H_{17}ClN_3S$, $[M+H]^+$). Anal. Calcd for $C_{20}H_{16}ClN_3S$: C, 65.65; H, 4.41; N, 11.48. Found: C, 65.94; H, 4.63; N, 12.74.

4.4.11. (*E*)-1-(4-(4-Bromobenzylideneamino)phenyl)-3-phenylthiourea (3s)

Yellow crystals, yield 76%, mp: 196–197 °C, ^{1}H NMR (300 MHz, DMSO-d_6, δ ppm): 7.13 (t, J = 7.32 Hz, 1H), 7.28–7.37 (m, 4H), 7.49 (d, J = 7.47 Hz, 2H), 7.54 (d, J = 8.76 Hz, 2H), 7.73 (d, J = 8.43 Hz, 2H), 7.88 (d, J = 8.61 Hz, 2H), 8.66 (s, 1H), 9.82 (d, J = 9.87 Hz, 2H). ESI-MS: 410.0 ($C_{20}H_{17}BrN_3S$, $[M+H]^+$). Anal. Calcd for $C_{20}H_{16}BrN_3S$: C, 58.54; H, 3.93; N, 10.24. Found: C, 58.34; H, 4.17; N, 10.55.

4.4.12. (*E*)-1-(4-(4-Nitrobenzylideneamino)phenyl)-3-phenylthiourea (3t)

Yellow crystals, yield 80%, mp: 196–197 °C, ^{1}H NMR (300 MHz, DMSO-d_6, δ ppm): 7.14 (t, J = 7.32 Hz, 1H), 7.32–7.40 (m, 4H), 7.49 (d, J = 7.68 Hz, 2H), 7.60 (d, J = 8.79 Hz, 2H), 8.19 (d, J = 8.94 Hz, 2H), 8.37 (d, J = 8.79 Hz, 2H), 8.86 (s, 1H), 9.87 (d, J = 11.52 Hz, 2H). ESI-MS: 377.1 ($C_{20}H_{17}N_4O_2S$, $[M+H]^+$). Anal. Calcd for $C_{20}H_{16}N_4O_2S$: C, 63.81; H, 4.28; N, 14.88. Found: C, 63.99; H, 4.56; N, 14.75.

4.4.13. (*E*)-1-(4-(4-Methylbenzylideneamino)phenyl)-3-phenylthiourea (3u)

Yellow crystals, yield 75%, mp: 170–171 °C, ^{1}H NMR (300 MHz, DMSO-d_6, δ ppm): 2.49 (s, 3H, CH_3), 7.13 (t, J = 7.32 Hz, 1H), 7.26 (d, J = 8.76 Hz, 2H), 7.31–7.36 (m, 4H), 7.51 (t, J = 8.96 Hz, 4H), 7.82 (d, J = 8.25 Hz, 2H), 8.60 (s, 1H), 9.80 (d, J = 10.23 Hz, 2H). ESI-MS: 346.1 ($C_{21}H_{20}N_3S$, $[M+H]^+$). Anal. Calcd for $C_{21}H_{19}N_3S$: C, 73.01; H, 5.54; N, 12.16. Found: C, 73.32; H, 5.77; N, 12.38.

4.4.14. (*E*)-1-(4-(4-(Benzyloxy)benzylideneamino)phenyl)-3-phenylthiourea (3v)

Yellow crystals, yield 79%, mp: 198–201 °C, ^{1}H NMR (300 MHz, DMSO-d_6, δ ppm): 5.20 (s, 2H, OCH_2), 7.14 (t, J = 10.15 Hz, 1H), 7.24 (d, J = 8.61 Hz, 2H), 7.31–7.41 (m, 6H), 7.47–7.53 (m, 7H), 7.89 (d, J = 8.79 Hz, 2H), 8.57 (s, 1H), 9.80 (d, J = 10.23 Hz, 2H). ESI-MS: 438.2 ($C_{27}H_{24}N_3OS$, $[M+H]^+$). Anal. Calcd for $C_{27}H_{23}N_3OS$: C, 74.11; H, 5.30; N, 9.60. Found: C, 74.42; H, 5.11; N, 9.78.

4.5. Crystal structure determination

Crystal structure determination of compound **3e** was carried out on a Nonius CAD4 diffractometer equipped with graphite-mono-chromated Mo Kα (λ = 0.71073 Å) radiation (Fig. 3). The structure was solved by direct methods and refined on F2 by full-matrix least-squares methods using SHELX-97.[33] All the non-hydrogen atoms were refined anisotropically. All the hydrogen atoms were placed in calculated positions and were assigned fixed isotropic thermal parameters at 1.2 times the equivalent isotropic U of the atoms to which they are attached and allowed to ride on their respective parent atoms. The contributions of these hydrogen atoms were included in the structure-factors calculations. The crystal data, data collection and refinement parameter for the compound **3e** are listed in Table 4.

4.6. Antimicrobial activity

The antibacterial activity of the synthesized compounds was tested against *B. subtilis*, *E. coli*, *P. aeruginosa* and *S. aureus* using MH medium (Mueller-Hinton medium: casein hydrolysate 17.5 g, soluble starch 1.5 g, beef extract 1000 mL). The MICs (minimum inhibitory concentrations) of the test compounds were determined by a colorimetric method using the dye MTT (3-(4,5-dimethylthiazol-2-yl)-2,5-diphenyl tetrazoliumbromide).[31] A stock solution of the synthesized compound (100 μg/mL) in DMSO was prepared and graded quantities of the test compounds were incorporated in specified quantity of sterilized liquid MH medium. A specified quantity of the medium containing the compound was poured into microtitration plates. Suspension of the microorganism was prepared to contain approximately 10^5 cfu/mL and applied to microtitration plates with serially diluted compounds in DMSO to be tested and incubated at 37 °C for 24 h. After the MICs were visually determined on each of the microtitration plates, 50 μL of PBS (phosphate buffered saline 0.01 mol/L, pH 7.4, $Na_2HPO_4{\cdot}12H_2O$ 2.9 g, KH_2PO_4 0.2 g, NaCl 8.0 g, KCl 0.2 g, distilled water 1000 mL) containing 2 mg of MTT/mL was added to each well. Incubation was continued at room temperature for 4–5 h. The content of each well was removed, and 100 μL of isopropanol containing 5% 1 mol/L HCl was added to extract the dye. After 12 h of incubation at room temperature, the optical density (OD) was measured with a microplate reader at 550 nm. The observed MICs are presented in Table 1.

4.7. *E. coli* FabH purification and activity assay

Full-length *E. coli* acyl carrier protein (ACP), acyl carrier protein synthase (ACPS) and β-ketoacyl-ACP synthase III (FabH) were individually cloned into pET expression vectors with an N-terminal His-tag (ACP, ACPS in pET19; FabH in pET28).

All proteins were expressed in *E. coli* strain BL21(DE3). Transformed cells were grown on Luria-Bertani (LB) agar plates supplemented with kanamycin (30 mg/mL). Sodium dodecyl

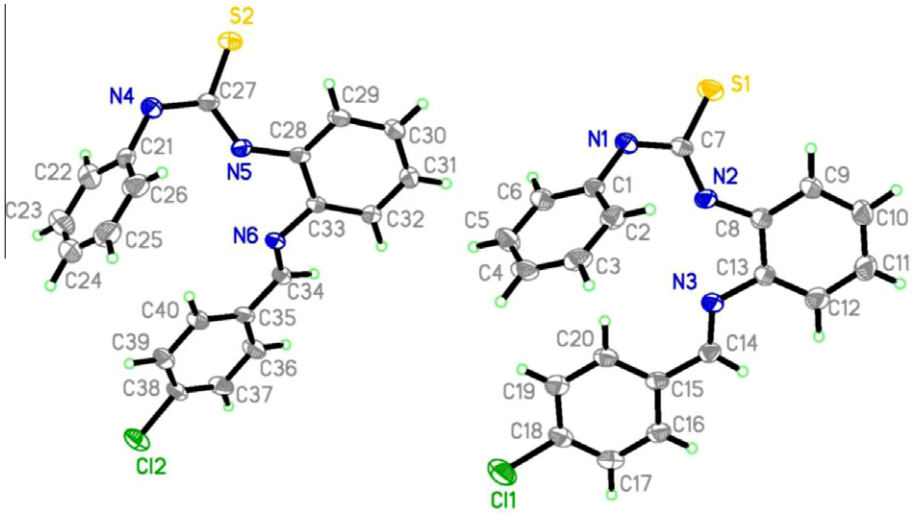

Figure 3. Crystal structure diagrams of compound **3e**. Molecule structure diagram with displacement ellipsoids being at the 30% probability level and H atoms are shown as small spheres of arbitrary radii.

Table 4
Crystallographical and experimental data for compound **3e**

Compound	**3e**
Empirical formula	$C_{20}H_{16}ClN_3S$
Formula weight	363.85
Crystal system	Monoclinic
Space group	*P*2(1)/*n*
a (Å)	8.4640(17)
b (Å)	23.169(5)
c (Å)	16.905(3)
α (°)	90.00
β (°)	100.33(3)
γ (°)	90.00
V (Å)	3261.4(11)
Z	8
D_{calc} (g cm^{-3})	1.482
θ range (°)	2.14–31.27
F(0 0 0)	1504
Reflections collected/unique	30,869/8846 [R_{int} = 0.0287]
Data/restraints/parameters	8846/0/451
Absorption coefficient (mm^{-1})	0.370
R_1; wR_2 [$I > 2\sigma(I)$]	0.0621/0.1427
R_1; wR_2 (all data)	0.1404/0.1758
GOOF	1.004

sulfate–polyacrylamide gel electrophoresis (SDS–PAGE) analysis was used to screen colonies for overexpression of proteins. One such positive colony was used to inoculate 10 mL of LB medium with 30 mg/mL of kanamycin and grown over night at 37 °C, 1 mL of which was used to inoculate 100 mL LB medium supplemented with 30 μg/mL of kanamycin. The culture was shaken for 4 h at 37 °C, and then induced with 0.5 mM isopropyl β-D-thiogalactopyranoside (IPTG). The culture was grown for 4 h, and harvested by centrifugation (30 min at 15,000 rpm).

Harvested cells containing His-tagged ACP, ACPS and FabHs were lysed by sonication in 20 mM Tris, pH 7.6, 5 mM imidazole, 0.5 M NaCl and centrifuged at 20,000 rpm for 30 min. The supernatant was applied to a Ni-NTA agarose column, washed and eluted using a 5–500 mM imidazole gradient over 20 column volumes. Eluted protein was dialyzed against 20 mM Tris, pH 7.6, 1 mM DTT and 100 mM NaCl. Purified FabHs were concentrated up to 2 mg/mL and stored at −80 °C in 20 mM Tris, pH 7.6, 100 mM NaCl, 1 mM DTT and 20% glycerol for enzymatic assays.

Purified ACP contains the apo-form that needs to be converted into the holo-form. The conversion reaction is catalyzed by ACP synthase (ACPS). In the final volume of 50 mL, 50 mg ACP, 50 mM Tris, 2 mM DTT, 10 mM $MgCl_2$, 600 μM CoA and 0.2 μM ACPS was incubated for 1 h at 37 °C. The pH of the reaction was then adjusted to approximately 7.0 using 1 M potassium phosphate. Holo-ACP was purified by fractionation of the reaction mixture by Source Q-15 ion exchange chromatography using a 0–500 mM NaCl gradient over 2 column volumes.

In a final 20 μL reaction, 20 mM Na_2HPO_4/NaH_2PO_4, pH 7.0, 0.5 mM DTT, 0.25 mM $MgCl_2$ and 2.5 mM holo-ACP were mixed with 1 nM FabH, and H_2O was added to 15 μL. After 1 min incubation, a 2 μL mixture of 25 μM acetyl-CoA and 0.75 μCi [^{3}H] acetyl-CoA was added for FabH reaction for 25 min. The reaction was stopped by adding 20 μL of ice-cold 50% TCA, incubating for 5 min on ice, and centrifuging to pellet the protein. The pellet was washed with 10% ice-cold TCA and resuspended with 5 μL of 0.5 M NaOH. The incorporation of the ^{3}H signal in the final product was read by liquid scintillation. When determining the inhibition constant (IC_{50}), inhibitors were added from a concentrated DMSO stock such that the final concentration of DMSO did not exceed 2%.

4.8. Molecular docking modeling

The crystal structures of *E. coli* FabH (PDB code: 1HNJ)[32] was obtained from the Protein Data Bank (http://www.rcsb.org).

Studies were carried out on only one subunit of the enzymes. The graphical user interface AutoDockTools (ADT) was employed to setup the enzymes: all hydrogens were added, Gasteiger charges were calculated and nonpolar hydrogens were merged to carbon atoms. For macromolecules, generated pdbqt files were saved.

The 3D structures of ligand molecules were built, optimized (PM3) level, and saved in mol2 format with the aid of the molecular modeling program Spartan (Wavefunction Inc.). These partial charges of Mol2 files were further modified by using the ADT package (version 1.4.6) so that the charges of the nonpolar hydrogens atoms assigned to the atom to which the hydrogen is attached. The resulting files were saved as pdbqt files.

AutoDock 4.0 was employed for all docking calculations.[34,35] The AutoDockTools program was used to generate the docking input files. In all docking a grid box size of 48 × 48 × 48 points in *x*, *y* and *z* directions was built in the catalytic site of the protein. A grid spacing of 0.375 Å (approximately one forth of the length of carbon–carbon covalent bond) and a distances-dependent function of the dielectric constant were used for the calculation of the energetic map. Ten runs were generated by using Lamarckian genetic

algorithm searches. Default settings were used with an initial population of 50 randomly placed individuals, a maximum number of 2.5×10^6 energy evaluations, and a maximum number of 2.7×10^4 generations. A mutation rate of 0.02 and a crossover rate of 0.8 were chosen. Results differing by less than 0.5 Å in positional root-mean-square deviation (RMSD) were clustered together and the results of the most favorable free energy of binding were selected as the resultant complex structures.

Acknowledgment

This work was supported by Jiangsu National Science Foundation (No. BK2009239) and the Fundamental Research Funds for the Central Universities (No. 1092020804 & 1106020824).

References and notes

1. Leeb, M. *Nature* **2004**, *431*, 892.
2. Cronan, J. E., Jr.; Rock, C. O. In *Escherichia coli and Salmonella typhimurium: Cellular and Molecular Biology*; Neidhardt, F. C., Ingraham, I. L., Low, K. B., et al., Eds.; American Society of Microbiology: Washington, DC, 1996; pp 612–638.
3. Khandekar, S. S.; Daines, R. A.; Lonsdale, J. T. *Curr. Protein Pept. Sci.* **2003**, *4*, 21.
4. Heath, R. J.; Rock, C. O. *Nat. Prod. Rep.* **2002**, *19*, 581.
5. Tsay, J. T.; Oh, W.; Larson, T. J.; Jakowski, S.; Rock, C. O. *J. Biol. Chem.* **1992**, *267*, 6807.
6. Clough, R. C.; Matthis, A. L.; Barnum, S. R.; Jaworski, J. G. *J. Biol. Chem.* **1992**, *267*, 20992.
7. Heath, R. J.; Rock, C. O. *J. Biol. Chem.* **1996**, *271*, 1833.
8. White, S. W.; Zheng, J.; Zhang, Y. M.; Rock, C. O. *Annu. Rev. Biochem.* **2005**, *74*, 791.
9. Veyron-Churlet, R.; Guerrini, O.; Mourey, L.; Daffé, M.; Zerbib, D. *Mol. Microbiol.* **2004**, *54*, 1161.
10. Christensen, C. E.; Kragelund, B. B.; von Wettstein-Knowles, P.; Henriksen, A. *Protein Sci.* **2007**, *16*, 261.
11. Bylka, W.; Matlawska, I.; Pilewski, N. A. *JANA* **2004**, *7*, 24.
12. Huycke, M. M.; Sahm, D. F.; Gilmore, M. S. *Emerg. Infect. Dis.* **1998**, *4*, 239.
13. Lee, P. J.; Bhonsle, J. B.; Gaona, H. W.; Huddler, D. P.; Heady, T. N.; Kreishman-Deitrick, M.; Bhattacharjee, A.; McCalmont, W. F.; Gerena, L.; Lopez-Sanchez, M.; Roncal, N. E.; Hudson, T. H.; Johnson, J. D.; Prigge, S. T.; Waters, N. C. *J. Med. Chem.* **2009**, *52*, 952.
14. Nie, Z.; Perretta, C.; Lu, J.; Su, Y.; Margosiak, S.; Gajiwala, K. S.; Cortez, J.; Nikulin, V.; Yager, K. M.; Appelt, K.; Chu, S. *J. Med. Chem.* **2005**, *48*, 1596.
15. Daines, R. A.; Pendrak, I.; Sham, K.; Aller, G. S. V.; Konstantinidis, A. K.; Lonsdale, J. T.; Janson, C. A.; Qiu, X.; Brandt, M.; Khandekar, S. S.; Silverman, C.; Head, M. S. *J. Med. Chem.* **2003**, *46*, 5.
16. Asheka, A.; Cho, S. J. *Bioorg. Med. Chem.* **2006**, *14*, 1474.
17. Singh, S.; Soni, L. K.; Gupta, M. K.; Prabhakar, Y. S.; Kaskhedikar, S. G. *Eur. J. Med. Chem.* **2008**, *43*, 1071.
18. Shi, L.; Ge, H.-M.; Tan, S.-H.; Li, H.-Q.; Song, Y.-C.; Zhu, H.-L.; Tan, R.-X. *Eur. J. Med. Chem.* **2007**, *42*, 558.
19. Huang, G. S.; Liang, Y. M.; Wu, X. L.; Liu, W. M.; Ma, Y. X. *Appl. Organo-met. Chem.* **2003**, *17*, 706.
20. Curini, M.; Epifano, F.; Maltese, F.; Marcotullio, M. C. *Tetrahedron Lett.* **2002**, *43*, 3821.
21. Yadav, L. D. S.; Yadav, B. S.; Rai, V. K. *Tetrahedron Lett.* **2004**, *45*, 5351.
22. Zhang, L. X.; Liu, Y.; Cia, L. H.; Hu, Y. J.; Yin, J.; Hu, P. Z. *Thermochim. Acta* **2006**, *440*, 51.
23. Lee, J.-Y.; Jeong, K.-W.; Lee, J.-U.; Kang, D.-I.; Kim, Y. *Bioorg. Med. Chem.* **2009**, *17*, 1506.
24. Nakano, H.; Haroda, H.; Funaoka, T.; Akashi, K. *Chem. Abstr.* **1973**, *78*, 43086.
25. Pluempe, H.; Pulls, W. *Chem. Abstr.* **1971**, *74*, 1251154n.
26. Salman, A. K.; Neha, S.; Kishwar, S. *Eur. J. Med. Chem.* **2008**, *43*, 2272.
27. Yonova, P. A.; Stoilkova, G. M. *J. Plant Growth Regul.* **2004**, *23*, 280.
28. Wang, J. D.; Martell, A. E.; Motekaitis, R. J.; Reibenspies, J. H. *Inorg. Chin. Acta* **2001**, *24*, 194.
29. Singhb, B.; Srivastava, U. *Synth. React. Inorg. Met. Org. Chem.* **1989**, *19*, 279.
30. Iskander, M. F.; El-Sayed, L.; El-Toukhy, A. C. *J. Inorg. Nucl. Chem.* **1980**, *42*, 145.
31. Meletiadis, J.; Meis, J. F.; Mouton, J. W.; Donnelly, J. P.; Verweij, P. E. *J. Clin. Microbiol.* **2000**, *38*, 2949.
32. Qiu, X.; Janson, C. A.; Smith, W. W.; Head, M.; Lonsdale, J.; Konstantinidis, A. K. *J. Mol. Biol.* **2001**, *307*, 341.
33. Sheldrick, G. M. *Acta Crystallogr.* **2008**, *A64*, 112.
34. Morris, G. M.; Goodsell, D. S.; Halliday, R. S.; Huey, R.; Hart, W. E.; Belew, R. K.; Olson, A. J. *J. Comput. Chem.* **1998**, *19*, 1639.
35. Huey, R.; Morris, G. M.; Olson, A. J.; Goodsell, D. S. *J. Comput. Chem.* **2007**, *28*, 1145.